Polymer 50 (2009) 553–559

Contents lists available at ScienceDirect

Polymer

journal homepage: www.elsevier.com/locate/polymer

Effect of SiO_2 nanoparticle addition on the characteristics of a new organic–inorganic hybrid membrane

Shuili Yu [a,b,*], Xingtao Zuo [a], Ruiling Bao [a], Xia Xu [a], Juan Wang [a], Jun Xu [a]

[a] State Key Laboratory of Urban Water Resource and Environment, Harbin Institute of Technology, Harbin 150090, China
[b] State Key Laboratory of Pollution Control and Resource Reuse, Tongji University, Shanghai 200092, China

ARTICLE INFO

Article history:
Received 30 July 2008
Received in revised form
15 October 2008
Accepted 14 November 2008
Available online 21 November 2008

keywords:
Organic–inorganic hybrid membrane
Transport property
SiO_2 nanoparticle

ABSTRACT

Poly(vinylidene fluoride) composite membranes filled with different weight fractions of SiO_2 nanoparticles have been prepared by a blending method. Cation-exchange groups were introduced by the copolymerization of glycidyl methacrylate with divinylbenzene and subsequent sulfonation. These hybrid membranes have been characterized by Fourier-transform infrared (FTIR) spectroscopy, scanning electron microscopy (SEM), differential scanning calorimetry (DSC), and water uptake and ion-exchange capacity measurements. Membrane potential and membrane conductivity measurements have been carried out with different counter ions to investigate the relationship between ionic migration and the SiO_2 nanoparticle content. The counter-ion transport number and permselectivity of these membranes are found to be highly dependent on the SiO_2 content in the membrane phase and the nature of the counter ion. Membrane conductance was analyzed in terms of phenomenological coefficients using non-equilibrium thermodynamic principles. It can be concluded that these hybrid membranes exhibit high thermal stability, improved selectivity, and moderate membrane conductivity, and may be suitable for use in the electro-driven separation processes.

1. Introduction

Various kinds of electro-membrane processes have been widely used in electrodialysis [1,2], diffusion dialysis, electrodeionization [3,4], membrane electrolysis [5,6], and fuel-cell-based electrochemical synthesis [7–9]. Predicting the efficiency of membranes in these processes requires a lot of information on the electrochemical properties of the solvent and the relevant ions in the membrane phase. The characteristics of the separation of specific ions from a given mixture are highly dependent on the size of the ions and the number of surrounding water molecules, and thus it is necessary to provide information about the ion–ion, ion–water, and ion–polymer interactions [10]. In this sense, the ion-exchange or membrane-transport characteristics would be more relevant to the polymer structure, and such knowledge would be very useful in establishing polymer design concepts for practical applications [11]. In addition, the electro-kinetic properties of a membrane have been proved to be a major factor in determining its applicability for a specific separation process [12]. It is well documented that the surface charge on a polymer membrane has a significant influence on its separation properties [13,14]. Previous reports [15,16] provide a basis for an investigation of different physicochemical and electrochemical parameters of ion-exchange membranes, with a view to predicting their performances and assessing their suitability for various electrochemical and separation processes by applying non-equilibrium thermodynamic principles.

The development of chemically and thermally stable ion-exchange membranes with good physicochemical and electrochemical properties that show specific selectivity is highly desirable. In this context, poly(vinylidene fluoride) (PVDF) is an excellent material that can form asymmetric membranes. Furthermore, PVDF has a high dielectric constant ($\varepsilon = 8.4$) and the strong electron-withdrawing functional group (–C–F–). It can be swollen in carbonate but not solvated [17,18], and it may provide a supporting structural phase with good mechanical strength when used as the polymer matrix for membranes. In many studies, attempts have been made to improve the performance of PVDF membranes by using various techniques, including physical blending, chemical grafting, and surface modifications [19–21].

The addition of inorganic fillers has led to increased membrane permeability and improved control of membrane surface properties [22]. Inorganic materials that can be blended with PVDF include silica, Al_2O_3, Fe_3O_4, ZrO_2, TiO_2, and polymeric nanoparticles. The morphology and elasticity of PVDF membranes are significantly affected by the weight ratio of added inorganic materials [23]. It has also been reported [24,25] that PVDF is

* Corresponding author. Tel./fax: +86 451 8628 2101.
E-mail address: ysl@vip.163.com (S. Yu).

0032-3861/$ – see front matter © 2008 Elsevier Ltd. All rights reserved.
doi:10.1016/j.polymer.2008.11.012

a common ultrafiltration, microfiltration, and pervaporation membrane material. However, very little work has been carried out on the preparation and application of PVDF–nanostructure inorganic composite materials as ion-exchange membranes. It is expected that ion-exchange membranes based on PVDF–inorganic composites may exhibit excellent thermal, mechanical, and electrochemical properties, as a result of the inherent properties of both components.

In this work, PVDF ion-exchange membranes have been prepared with inorganic SiO_2 nanoparticles at different weight fractions. Cation-exchange groups were introduced into the membrane matrix by reaction of the epoxy groups of glycidyl methacrylate (GMA) with fuming sulfuric acid at 25 °C. These membranes are designated as PVDF/GMA/SiO_2-*X*, where *X* is the weight ratio of SiO_2 nanoparticles in the membrane-forming materials. The effects of the SiO_2 content in the membrane matrix on the morphology and thermal properties of the membrane have been examined. Their transport properties were studied in electrolyte solutions of different concentrations to investigate the relationship between ionic migration and SiO_2 nanoparticle content.

2. Experimental

2.1. Materials

Poly(vinylidene fluoride) (PVDF) used in this study was a commercial product (FR904) (Shanghai 3F New Materials Co., Ltd.). Nanosized SiO_2 particles (30 nm) (Zhejiang Mingri Chemicals Co., China) were used as an additive for PVDF solutions. Glycidyl methacrylate (GMA) was supplied by Shanghai YuanJi Chemical Ltd., China, and was used without further purification. Divinylbenzene (DVB) was purchased from Qingshengda Chemical Ltd., China. Dimethylacetamide (DMAC, >99%), benzoyl peroxide (BPO), fuming sulfuric acid, HCl, NaOH, NaCl, $MgCl_2$, and $CaCl_2$ (Tianjin Chemical Reagents Plant, China) all were of AR grade. Doubly distilled water was used for the preparation of all the solutions.

2.2. Membrane preparation

PVDF/GMA/SiO_2 hybrid membranes were prepared with different contents of SiO_2 nanoparticles by a conventional casting method. Viscous slurries were obtained by mixing PVDF, SiO_2, BPO, DVB, and GMA in DMAC at a fixed PVDF:DMAC ratio of 1:3 (w/w). The various SiO_2 contents were 0, 0.07, 0.14, 0.21, and 0.28 wt% based on the total weight of the PVDF/GMA/SiO_2 hybrid membranes. The resulting mixtures were left to stand for 24 h to remove air bubbles and to obtain gels, and then cast on clean glass plates by using a doctor blade. The resulting membranes were dried at 100 °C for 2 h to introduce crosslinking. The obtained membranes were immersed in fuming sulfuric acid at room temperature for 3 days, and then washed with distilled water until all traces of acidity were removed. The PVDF/GMA/SiO_2 membranes were stored in deionized water before use. The membrane thickness was in the range 0.19–0.25 mm.

2.3. Characterization of the polymer membranes

2.3.1. Scanning electron microscopy (SEM)

The surface and cross-section morphologies of the membranes were analyzed by means of scanning electron microscopy (S4800HSD, Japan). Cross-sections of the membranes were obtained by breaking the samples in liquid nitrogen. Gold sputter coatings were applied to the membrane samples of interest at pressures between 1 and 0.1 Pa.

2.3.2. FTIR

Infrared spectra of the membranes were recorded under nitrogen atmosphere on a Perkin Elmer FTIR 1710 spectrometer (Japan), covering a range of 500–4000 cm^{-1} with a resolution of 2 cm^{-1}.

2.3.3. Thermal stabilities

Thermal stability of the membranes was determined by thermogravimetric analysis (TGA) (Netzsch STA 449C, Germany). In order to remove the residual solvent from the membranes, 5–10 mg specimens were kept at 60 °C for 20 min under vacuum (100 mmHg column) and then heated under N_2 atmosphere from 80 to 800 °C at 10 °C min^{-1}.

2.3.4. Water content

The hybrid membranes were completely soaked in water for 24 h to ensure saturation. The excess water was removed by gently wiping it off with a filter paper and the wet membrane samples were weighed. The samples were then dried under vacuum at 60 °C (100 mmHg column) to completely remove the water and weighed again until a constant weight was obtained. The water content of the membrane was determined from the weight difference before and after hydration.

2.3.5. Membrane potential and conductance

The experimental cell used for membrane potential measurements [26] had two compartments separated by a membrane of circular shape with an effective area of 7.0 cm^2. To minimize the effect of boundary layers on potential, the solutions in the compartments were vigorously stirred by means of magnetic stirrers. The potential difference that developed across the membrane was recorded by a multimeter using saturated calomel electrodes and salt bridges, and the measurements were found to be reproducible within 0.10 mV. For membrane potential measurements, the ratio of salt concentrations on the higher and lower sides (C_1/C_2) was kept constant at 10 ($\Delta C/C_s = 1.64$), where C_1 and C_2 are the electrolyte concentrations, $\Delta C = C_1 - C_2$, and $C_s = (C_1 + C_2)/2$.

Membrane conductance measurements for different composite membranes were carried out using a cup cell, as reported previously in the literature [26]. The cell was composed of two black graphite electrodes fixed on Plexiglass plates. The active area of the electrodes as well as that of the membrane was 1.0 cm^2. During the experiments, the equilibrated membrane in the experimental solution was sandwiched between the two electrodes and secured in place by means of a set of screws. Membrane conductance measurements were performed in potentiostatic two-electrode mode with alternating current (AC). Membrane resistance (R_m) was estimated by subtraction of the electrolyte resistance (R_{sol}) without a membrane from the membrane resistance in equilibrated electrolyte solutions (R_{cell}) ($R^m = R_{cell} - R_{sol}$). The membrane conductance was measured by using a digital conductivity meter with up to ±0.01 mS reproducibility. The specific conductivity of the membrane was estimated by means of the following equation:

$$\kappa = \frac{l}{AR^m} \tag{1}$$

where *l* is the thickness of the wet membrane, *A* is its area, and R^m is its resistance.

3. Results and discussion

3.1. Morphology

In order to study the effect of SiO_2 nanoparticles on the microstructure of the membranes, SEM micrographs of the surfaces and

cross-sections of PVDF/GMA/SiO_2 membranes with different SiO_2 contents were obtained. It became clear that the changes in the SEM surface and cross-section images of the five types of membranes followed a regular trend with increasing SiO_2 content; therefore, as representative examples, only the SEM images of PVDF/GMA/SiO_2-X ($X = 0$, 0.14, and 0.28) hybrid membranes are illustrated in Fig. 1.

As is clear from Fig. 1(a–c), no phase separation at the surfaces of the PVDF/GMA/SiO_2 membranes can be observed, indicating that these membranes are homogeneous in nature, while the surface morphologies of these membranes gradually become smoother and denser as the SiO_2 content in the membrane matrix is increased. In addition, the particle size of the SiO_2 is seen to range from several nm to around 100 nm, which suggests that the prepared membranes can be considered as PVDF–SiO_2 nanocomposites. From the cross-section images of these membranes shown in Fig. 1(d–f), it can clearly be observed that the cross-sectional microstructures of these membranes become denser with increasing SiO_2 content. Moreover, the pores and voids in the cross-section become smaller and smaller as compared to the flaky surface with unevenly sized pores. These differences in the SEM morphologies of the membranes reflect the effect of SiO_2 nanoparticles on their microstructures. These results may be due to the establishment of higher crosslinking density in the inorganic–organic networks as the formation of one network has a significant effect on the formation of the other.

3.2. FTIR studies

Fig. 2 shows the FTIR spectra of PVDF/GMA/SiO_2-X hybrid membranes with $X = 0$, 0.14, and 0.28. Strong absorption peaks associated with the $-CH_3$ or $-CH_2-$ groups are observed at $\nu = 2940\ cm^{-1}$. A distinct absorption peak at $\nu = 1710\ cm^{-1}$ may be assigned to the stretching vibration of the –C–F functional

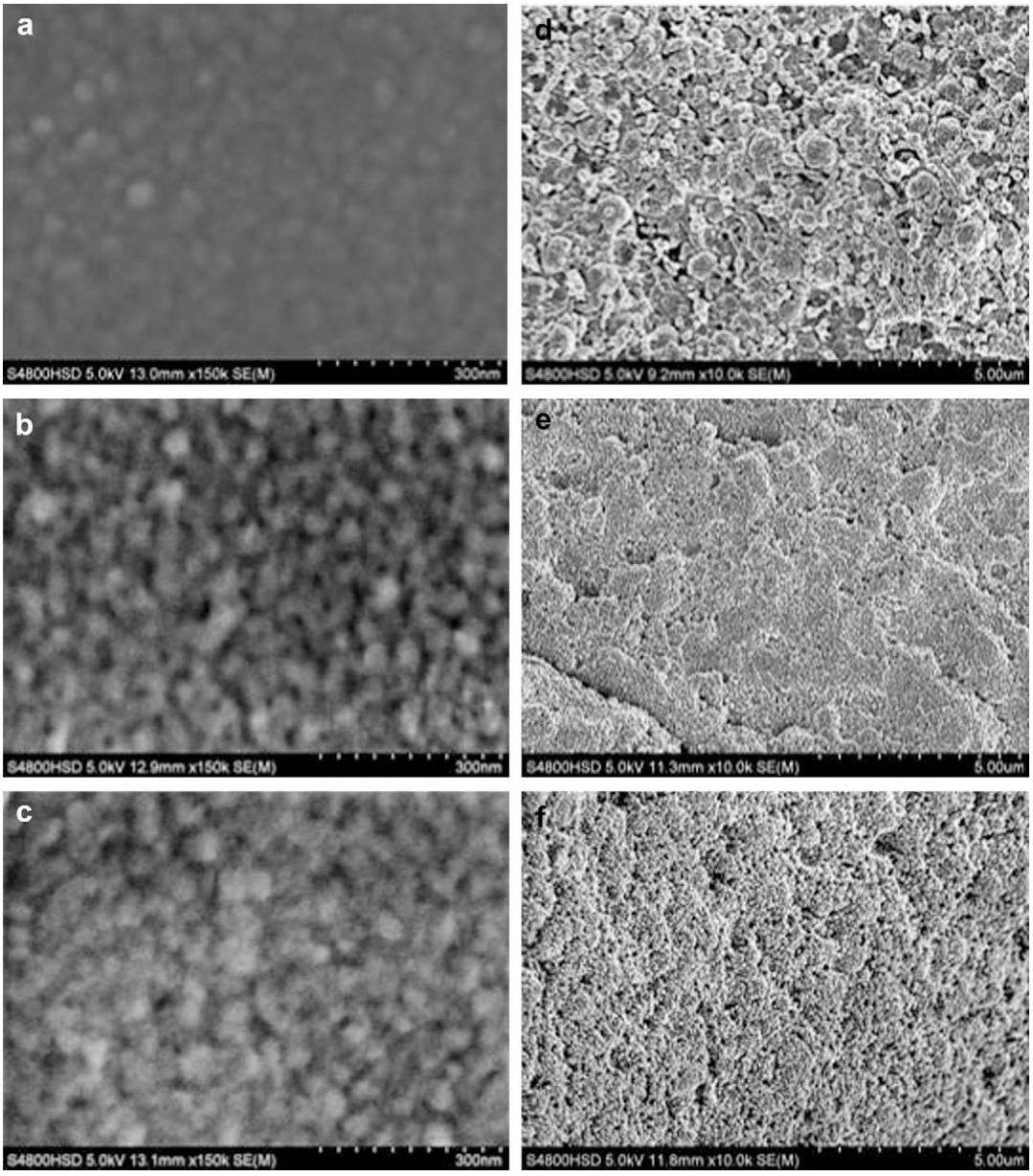

Fig. 1. SEM images of the surface of the PVDF/GMA/SiO_2-X hybrid membranes: (a) $X = 0$, (b) $X = 0.14$, (c) $X = 0.28$. SEM images of cross-section of the hybrid membranes: (d) $X = 0$, (e) $X = 0.14$, (f) $X = 0.28$.

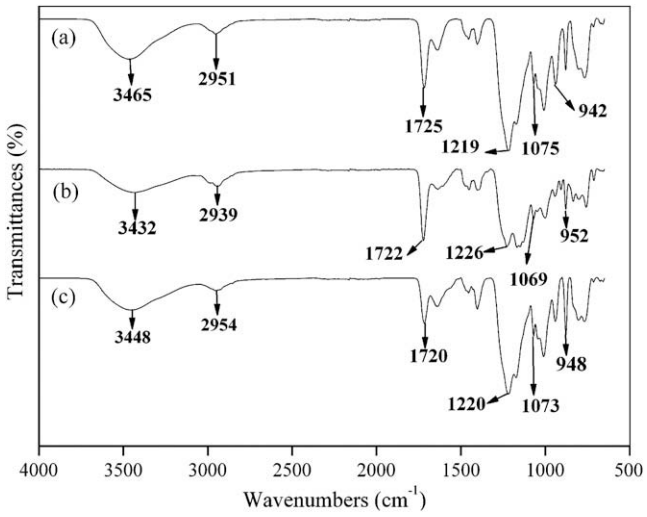

Fig. 2. FTIR spectra for (a) PVDF/GMA/SiO_2-0; (b) PVDF/GMA/SiO_2-0.14; (c) PVDF/GMA/SiO_2-0.28.

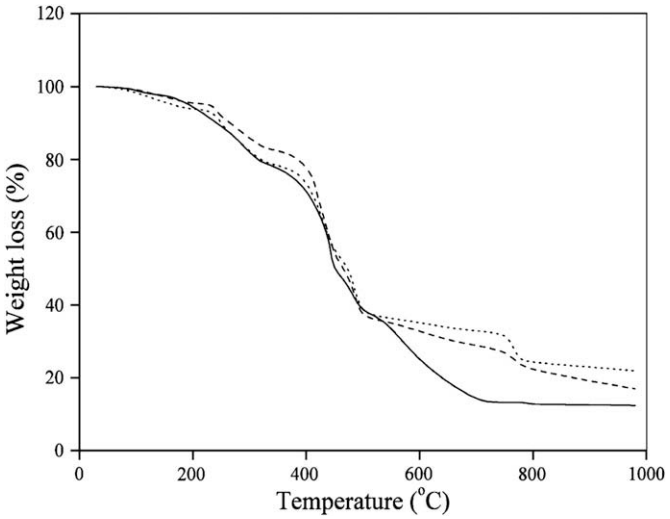

Fig. 3. TGA curves of the hybrid membranes for (—) PVDF/GMA/SiO_2-0; (– – –) PVDF/GMA/SiO_2-0.14; (……) PVDF/GMA/SiO_2-0.28.

group, while the intensity in the region of $\nu = 950\ cm^{-1}$ may be attributed to –SiOH stretches, which increases with the weight fraction of SiO_2 particles in the membrane matrix. Since the characteristic peaks of $-SO_3H$ groups at $\nu = 1100\ cm^{-1}$ overlap with the Si–O–C and Si–O–Si stretching bands, they cannot be distinguished. The ion-exchange capacity discussed in the following section confirms the formation of $-SO_3H$ groups during the sulfonation process.

Due to the complexity of the spectra, differences in the intensities of the inorganic Si–O–Si bands and the organic C–O–C bands among the hybrid materials cannot be clearly distinguished. The intensities of the peaks attributable to the epoxy ring of GMA at $\nu = 1254$, 909, and 821 cm^{-1} are decreased, revealing partial opening of the epoxy rings but that some of them remain intact. The broad –OH absorption peak observed for membranes with $X = 0.14$, 0.28 at around 3400 cm^{-1} indicates a significant contribution from the –SiOH or –OH groups of GMA after sulfonation.

3.3. Thermal properties

The thermal stabilities of the membranes were investigated by TGA and the obtained diagrams are shown in Fig. 3. Thermal stability parameters, including initial decomposition temperature (IDT) and thermal degradation temperature at 5% weight loss (T_d), were determined from the TGA thermograms. It is clear that the IDT value of the hybrid membrane without SiO_2 is 190 °C, while the values for the membranes loaded with SiO_2 are all higher than 220 °C. Increasing SiO_2 content in the membrane phase leads to increased IDT values, as shown in Fig. 3. The T_d values are in the range 220–300 °C, indicating that these membranes prepared with SiO_2 particles can endure relatively high temperatures. There is no obvious increasing or decreasing trend in the T_d values of these hybrid membranes. However, it should be noted that the T_d values of these membranes increase with increasing SiO_2 content in the membrane matrix. These results are consistent with the observation that the thermal stabilities of the hybrid materials increase with increasing inorganic silica content [27]. In addition, the presence of SiO_2 in the membrane-forming materials strengthens the inorganic silica network of the hybrid membranes, thereby leading to a corresponding enhancement in their thermal stabilities.

3.4. Electrochemical properties of the cation-exchange membranes

3.4.1. Water content and ion-exchange capacity (IEC)

There are two distinct factors that influence the water content of a membrane, namely its chemical structure and the nature and concentration of the electrolyte solution in contact with it. The water contents of the different types of membranes are plotted in Fig. 4. It is clearly evident that the water content increases with increasing SiO_2 nanoparticle content. The densities of ionizable groups in these hybrid membranes are changed, which may be responsible for the observed variation in water content. Furthermore, the incorporation of more SiO_2 nanoparticles into the membrane matrix may also lead to an increase in pore volume and thus water uptake. A further reason may be that these –OH groups provide sites for hydrogen bonding between the polymer and water, because the SiO_2 nanoparticles are observed to retain water, even at high temperatures [28].

The cation-exchange capacities of the composite membranes were determined by the conventional method [29], in which the hybrid materials in their H^+ ionic form were neutralized with NaOH and then back-titrated with 0.01 mol dm^{-3} HCl. Ion-exchange

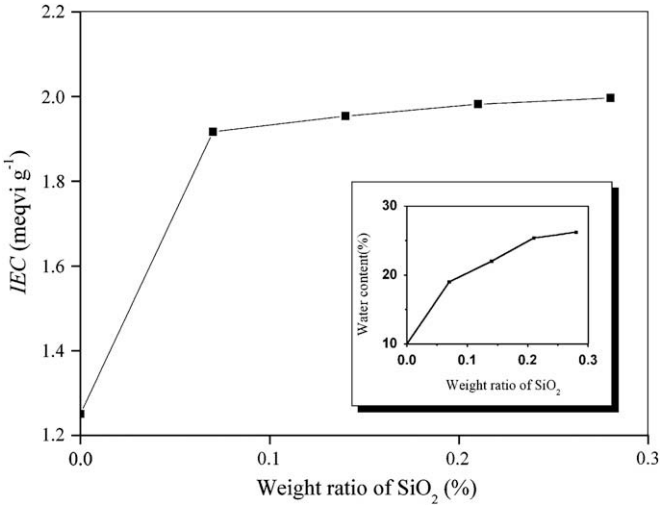

Fig. 4. Variation of IEC for different types of membranes.

capacity indicates the density of ionizable hydrophilic groups in the membrane matrix, which is responsible for the ionic conductivity in the ion-exchange membrane [30]. The IEC values of all of the prepared membranes are also presented in Fig. 4. As can be seen, IEC values increase with increasing silica content in the membrane matrix, and are in the range 1.2–2.0 mequiv. g^{-1}. It is inferred that the physicochemical properties of these membranes are improved with the addition of SiO_2, which will be discussed in the following sections, and thus the degree of sulfonation may be enhanced. It is noticeable that as the IEC values of these membranes increase, the membranes become more hydrophilic and absorb more water, as manifested in the increased measured water contents indicated in Fig. 4.

3.4.2. Membrane potential and membrane permselectivity

When electrolyte solutions of unequal concentrations are separated by a membrane, an electrical potential develops across the membrane due to the tendency of the cations to move with different velocities. The magnitude of the membrane potential depends on the electrical characteristics of the membrane along with the nature and concentration of the electrolyte solution used [31].

Membrane potential data for the present hybrid membranes prepared with different weight fractions of SiO_2 nanoparticles, which were obtained in NaCl solution at a mean concentration of 0.055 mol dm^{-3}, are presented in Fig. 5. It can be seen that the E^m values of these membranes are increased by the presence of SiO_2 nanoparticles. With an increase in the nanosized SiO_2 content, the surface charge density of ionic functional groups increases, resulting in enhanced Donnan exclusion, which contributes to the total potential developed across the membrane [32]. The Stokes radii for the different counter ions follow the trend $Na^+ < Mg^{2+} < Ca^{2+}$ [33], while the opposite trend is observed for the membrane potentials.

For a cation-exchange membrane, the membrane potential in the present case may be expressed by the following equation [34]:

$$E^m = (1 - 2t_+^m)\frac{RT}{F}\ln\frac{a_1}{a_2} \quad (2)$$

where a_1 and a_2 are the mean activities of the electrolyte solutions and t_+^m denotes the transport number of the cation in the membrane phase. Mean activity coefficients were estimated from the Debye–Hückel limiting law. The t_+^m values for the different types of membranes estimated by applying Eq. (2) are listed in Table 1. All

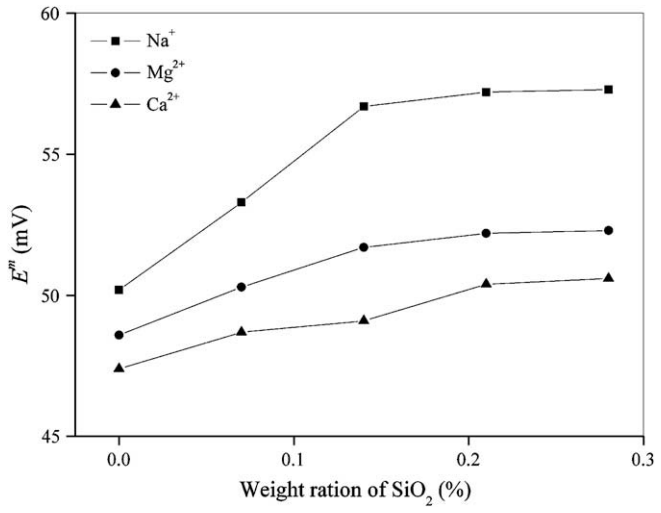

Fig. 5. Membrane potential values for PVDF/GMA/SiO_2 hybrid membranes in NaCl solution of 0.055 mol dm^{-3}.

Table 1
Cation-transport number and permselectivity values for different membranes in NaCl solution with different mean concentrations.

Membrane[a]	0.055		0.11		0.165	
SiO_2/PVDF/GMA-X	t_+^m	P_s	t_+^m	P_s	t_+^m	P_s
0.00	0.925	0.879	0.910	0.855	0.904	0.845
0.07	0.951	0.921	0.935	0.895	0.930	0.887
0.14	0.979	0.966	0.968	0.948	0.959	0.934
0.21	0.984	0.974	0.977	0.963	0.973	0.956
0.28	0.985	0.976	0.979	0.966	0.975	0.961

[a] X is the weight ratio of SiO_2 particles in the membrane-forming materials.

of these membranes exhibit very good selectivity for Na^+. It can clearly be seen that transport numbers for Na^+ decrease with increasing concentration of the NaCl solution, which is considered to be due to the decrease in Donnan exclusion. The hydrophilic nature of the membranes prepared with loadings of nanosized SiO_2 may be responsible for the differences in their ion selectivities.

The ion selectivity of an ion-exchange membrane may be quantitatively expressed in terms of permselectivity (P_s), which arises due to the capacity of the membrane for discrimination between counter ion and co ion, and is expressed as [34]:

$$P_s = \frac{t_+^m - t_+}{1 - t_+} \quad (3)$$

where t_+ is the cation-transport number in the solution phase. Permselectivity values obtained under different experimental conditions are also given in Table 1. These data reveal that the hybrid membranes display very good Na^+ selectivity, while their cation selectivity increases remarkably with increasing SiO_2 content. For these membranes, permselectivity follows a similar trend to the cation-transport numbers. The effect of SiO_2 nanoparticles on the permselectivity may be attributed to two factors: (i) the increase of membrane-fixed charge density increases with the addition of SiO_2, resulting in enhanced Donnan exclusion of cations, and (ii) the pore density of the organic–inorganic hybrid membrane increases with the incorporation of SiO_2 nanoparticles, which is also supported by water-uptake studies and SEM images. The increase in IEC also supports the observed variation in permselectivity under different experimental conditions.

3.4.3. Membrane conductivity

Membrane conductance was measured for these hybrid membranes equilibrated with NaCl solutions of concentrations in the range 0.01–0.10 mol dm^{-3}. The variation in the specific membrane conductivity K^m with concentration of the NaCl solution is plotted in Fig. 6.

Recent experimental studies have shown that the three crucial factors influencing ion-exchange membrane conductivity are the electrostatic interactions between cation and the fixed charges, the relative sizes of the mobile ions, and the membrane structural properties [16,35]. As shown in Fig. 6, the variation in the K^m values for the different PVDF/GMA/SiO_2 hybrid membranes reveals that the interaction of Na^+ ion with the membrane matrix increases with increasing SiO_2 content. The conductivities of the membranes incorporating silica are higher than that of the membrane without silica. Also, the incorporation of SiO_2 nanoparticles into the membrane matrix increases the water content of the membrane and thus increases the conductivity.

The strength of static electric interaction between the membrane-fixed ion-exchange groups and cations depends on the membrane surface charge density and the cation valence [36–39]. It is inferred that with the addition of SiO_2, the strength of the static electric interaction between the cations and the negatively charged fixed groups is increased, which may result in an increase in ion-

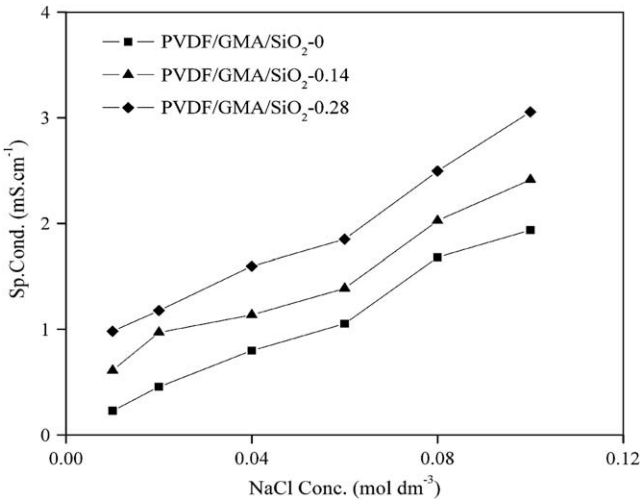

Fig. 6. Specific conductance values for different types of membranes at different concentrations of NaCl solution.

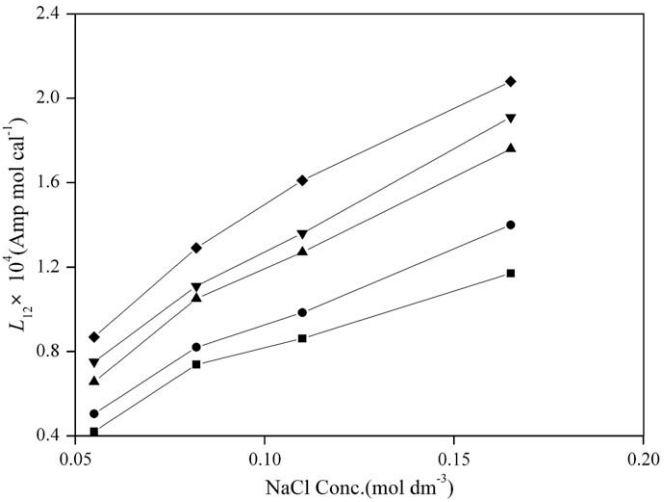

Fig. 8. L_{12} values for different hybrid membranes at different concentrations of NaCl solution: (■) $X = 0$; (●) $X = 0.07$; (▲) $X = 0.14$; (▼) $X = 0.21$; (◆) $X = 0.28$.

transfer resistance. Furthermore, the conductivity increases with an increase in fixed charge concentration [40], i.e. with increased cation concentration in the membrane phase. In addition, K^m values increase with increasing NaCl concentration as the cation concentration in the solution phase strongly influences the ion-transfer resistance. This is because an increase in solution concentration leads to increased screening of the attractive electrical interactions between cations and membrane groups, which decreases the static electric interaction strength.

The phenomenological coefficients describing current flow and solute flow occurring under the simultaneous action of a potential difference ($\Delta\phi$) and concentration difference (ΔC) may accordingly be written as [41]:

$$I = L_{11}\Delta\phi + L_{12}RT\frac{\Delta C}{C} \tag{4}$$

$$J_s = L_{21}\Delta\phi + L_{22}RT\frac{\Delta C}{C} \tag{5}$$

where L_{ij} ($i,j = 1, 2$) are the phenomenological coefficients. According to Eq. (4), L_{11} can be expressed by Eq. (6):

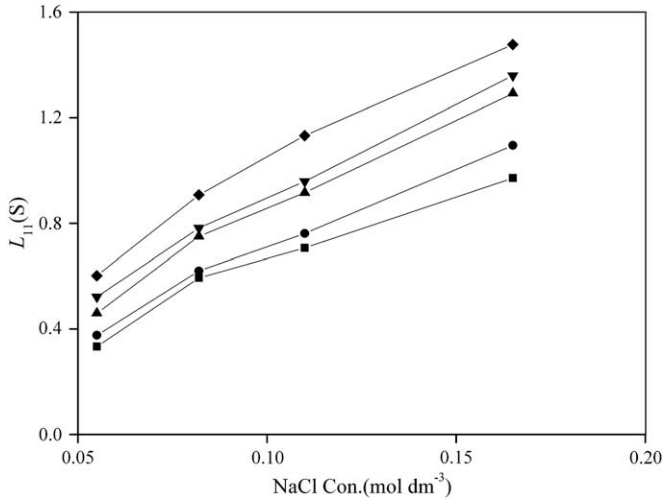

Fig. 7. L_{11} values for SiO_2/PVDF-X membranes at different concentrations of NaCl solution: (■) $X = 0$; (●) $X = 0.07$; (▲) $X = 0.14$; (▼) $X = 0.21$; (◆) $X = 0.28$.

$$\left(\frac{I}{\Delta\phi}\right)_{\Delta C=0} = L_{11} \tag{6}$$

Clearly, L_{11} represents the membrane conductance, and its values at different NaCl concentrations are plotted for different membranes in Fig. 7. The calculated values of L_{11} for different hybrid membranes increase with increasing concentration of the NaCl solution. These values also increase as the content of SiO_2 nanoparticles in the membrane matrix is increased, and follow a similar trend to K^m. Moreover, the trend in the L_{11} values also supports the explanation for K^m.

Membrane potential in combination with membrane conductance data can also be used for the estimation of L_{12}:

$$\left(\frac{\Delta\phi}{\Delta C}\right)_{I=0} = -\frac{L_{12}}{L_{11}}\frac{RT}{C} \tag{7}$$

Electro-driven solute migration across the membrane can be estimated using Onsager's reciprocal relationship $L_{12} = L_{21}$. This relationship is valid in all cases, and fluxes and forces are chosen on the basis of appropriate dissipation functions, which are linearly related [29]. Thus, L_{21} is a measure of electro-driven solute permeability. Fig. 8 shows the L_{12} values obtained from membrane potential and membrane conductance data for different membranes in NaCl solution. The L_{12} values increase with increasing SiO_2 weight ratio in the hybrid membrane matrix for all the NaCl solution concentrations. Meanwhile, the higher L_{11} value for Na^+ is responsible for higher solute flux. Furthermore, these observations also support the conclusion obtained on the basis of membrane potential studies.

4. Conclusions

An inorganic–organic hybrid membrane PVDF/GMA/SiO_2 has been developed for application in electro-membrane processes. FTIR, SEM, and TGA measurements have been conducted to characterize the properties and structures of these membranes. The cation-exchange membranes are physically stable up to 300 °C. The success of a sulfonation reaction between GMA and H_2SO_4 has been confirmed by IEC values in the range 1.2–2.0 mequiv. g^{-1}. The IEC values and measured water uptakes of these PVDF/GMA/SiO_2 hybrid membranes indicate that they have enhanced water-adsorbing and hydrophilic properties due to the presence of the

SiO_2 nanoparticles in the membrane matrix. These membranes incorporating SiO_2 nanoparticles exhibit higher permselectivity for monovalent and bivalent ions. The increase in the concentration of fixed ionic charges is responsible for the variation in permselectivity. The specific membrane conductivities of these hybrid membranes increase with increasing SiO_2 nanoparticle content in the membrane-forming material, possibly because of the formation of an inorganic–organic network that improves the diffusion of cations in the membrane matrix. Phenomenological coefficient data support the explanation of membrane conductivity and permselectivity. PVDF/GMA/SiO_2 hybrid membranes show conductivity and selectivity properties comparable to those of commercial membranes, and so may find application in electrodriven separation processes and fuel cells.

Acknowledgements

This research is supported by National High Technology Research and Development Program of China (863 Program) (No. 2006AA06Z303), Key Projects in National Science & Technology Pillar Program (No. 2006BAJ08B09), National Natural Science Foundation of China (No. 50778050) and Foundation for Innovative Research Groups of China (No. 50821002). We would also like to acknowledge International Science Editing (ISE) for their contribution to have our paper polished.

References

[1] Rodrigues MA, Amado FD, Bischoff MR, Ferreira CA, Bernardes AM, Ferreira JZ. Desalination 2008;227:241–52.
[2] Svetlozar V, Cristina M, Adrian O, Susana S, Maria R, Joao C. Desalination 2008;223:85–90.
[3] Ludmila M, Olga V, Boris K. Desalination 1999;124:125–30.
[4] Shahi VK, Thampy SK, Rangarajan R. Desalination 2001;133:245–58.
[5] Minagawa M, Tanioka A, Ramirez P, Mafe S. J Colloid Interface Sci 1997;188:176–82.
[6] Shahi VK, Thampy SK, Rangarajan R. J Membr Sci 2002;203:43–51.
[7] Kwang MK, Park NG, Kwang SR, Soon HC. Electrochim Acta 2006;51:5636–44.
[8] Stolarska M, Niedzicki L, Borkowska R, Zalewska A, Wieczorek W. Electrochim Acta 2007;53:1512–7.
[9] Zhang Y, Zhang HM, Bi C, Zhu XB. Electrochim Acta 2008;53:4100–2.
[10] Paddison SJ, Paul R, Zawodzinski TA. J Electrochem Soc 2000;147:617–8.
[11] Okadaa T, Arimurab N, Satoub H, Yuasab M, Kikuchic T. Electrochim Acta 2005;50:3569–75.
[12] Benavente J, Canas A. J Membr Sci 1999;156:241–50.
[13] Godjevargova TS, Dimov A, Vassileva N. J Membr Sci 1996;116:273–8.
[14] Reboiras MD. J Membr Sci 1996;109:55–63.
[15] Shahi VK, Thampy SK, Rangarajan R. React Funct Polym 2000;46:40–1.
[16] Nagarale RK, Gohil GS, Shahi VK, Trivedi GS, Rangarajan R. J Colloid Interface Sci 2004;277:162–71.
[17] Gen LJ, Bao KZ, Zhen YC, Chun FZ, You YX. Polymer 2007;48:6415–25.
[18] Chen NP, Liang H. Polymer 2004;45:2403–11.
[19] Luisa DV, Debora M, Alessandra DE, Enrico T, Marcella T, Silvia L. Polymer 2005;46:1754–8.
[20] Xue S, Yin GP. Polymer 2006;47:5044–9.
[21] Lu Y, Yu SL, Chai BX. Polymer 2005;46:7701–6.
[22] Khayet M, Villaluengaa JP, Valentin JL. Polymer 2005;46:9881–91.
[23] Cao XC, Ma J, Shi XH, Ren ZJ. Appl Surf Sci 2006;253:2005.
[24] Chen YW, Deng QL, Xiao JC, Nie HR, Wu LC, Zhou WH, et al. Polymer 2007;48:7604–13.
[25] Sato H, Norisuye T, Takemori T, Nomura S. Polymer 2007;48:5681–7.
[26] Shahi VK, Thampy SK, Rangarajan R. J Membr Sci 1999;158:77–83.
[27] Wu CM, Xu TW, Yang WH. J Solid State Chem 2004;177:1660–6.
[28] Nogami M, Nagao R, Wong C. J Phys Chem B 1998;102:5772.
[29] Ohya H, Paterson R, Nomura T, Mcfadzean S, Suzuki T, Kogure M. J Membr Sci 1995;105:103–12.
[30] Gohil GS, Nagarale RK, Binsu VV, Shahi VK. J Colloid Interface Sci 2006;298:845–53.
[31] Zabolosky VI, Nikonenko VV. J Membr Sci 1993;79:181–9.
[32] Nagarale RK, Shahi VK, Thampy SK, Rangarajan R. React Funct Polym 2004; 61:131–8.
[33] Katchalsky A, Curran PF. Non-equilibrium thermodynamics in biophysics. Cambridge, MA: Harvard University Press; 1965.
[34] Ohataki H. Hydration of ions. Tokyo: Kyoritsu; 1992.
[35] Okada T, Xie G, Meeg M. Electrochim Acta 1998;43:2141–55.
[36] Okada T, Satou H, Okuno M, Yuasa M. J Phys Chem B 2002;106:1270.
[37] Rolando G, Wolfgang S. Electrochim Acta 2000;45:2317–38.
[38] Nwal DA, Alexandrova S, Schaetzel P. Electrochim Acta 2003;48:2563–9.
[39] Sa SB, Huang HL. Colloids Surf A Physicochem Eng Aspects 2008;315:99–102.
[40] Jonathan E, Stjepan M, Roland K. Electrochim Acta 1996;41:2115–24.
[41] Lakshiminarayanaiah N. Transport phenomena in membranes. New York: Academic Press; 1969.